Am J Transl Res 2019;11(8):5261-5271
www.ajtr.org /ISSN:1943-8141/AJTR0091775

Original Article

Suitability of the use of an elastin matrix combined with bone morphogenetic protein for the repair of cranial defects

Renato de Moraes[1,2], Ana Maria de Guzzi Plepis[3], Virginia da Conceição Amaro Martins[3], Marco Antonio Hungaro Duarte[4], Murilo Priori Alcalde[4], Rogerio Leone Buchaim[5,6], Karina Torres Pomini[5], Eduardo Gomes Machado[1,2], Marcelo de Azevedo e Sousa Munhoz[1,2], Fernando Bento Cunha[1,2], Amanda Regina Alves Calegari[1], Amilton Iatecola[1,7], Samantha Ketelyn Silva[1], Marcelo Rodrigues da Cunha[1,2,7]

[1]Department of Morphology and Pathology, Medical College of Jundiai, São Paulo, Jundiaí 13202-550, SP, Brazil; [2]Interunit Postgraduate Program in Bioengineering (EESC/FMRP/IQSC), University São Paulo, USP, São Carlos 3566-590, SP, Brazil; [3]Institute of Chemistry of São Carlos, University of São Paulo, USP, São Carlos 13566-590, SP, Brazil; [4]Department of Dentistry, Endodontics and Dental Materials, Bauru School of Dentistry, University of São Paulo, Bauru 17012901, SP, Brazil; [5]Department of Biological Sciences, Bauru School of Dentistry, University of São Paulo, Bauru 17012901, SP, Brazil; [6]Postgraduate Program in Structural and Functional Interactions in Rehabilitation, University of Marilia (UNIMAR), Marília 17525-902, SP, Brazil; [7]Laboratory of Anatomy, University Center Our Lady of Patronage, CEUNSP, University of South Cruise, Itu 13300-200, SP, Brazil

Received January 24, 2019; Accepted July 17, 2019; Epub August 15, 2019; Published August 30, 2019

Abstract: The use of biomaterials in medical and dental areas has become increasingly important due to the need to restore areas with bone loss or defects. This study analyzed the use of a new elastin polymer matrix combined with Bone Morphogenetic Protein for the repair of cranial defects in rats. Thirty rats were divided into five groups: control (C) defect without graft, E24 (defect filled with elastin matrix submitted to alkaline hydrolysis at 50°C for 24 h), E24/BMP (defect filled with elastin matrix treated at 50°C for 24 h plus BMP), E96 (defect filled with elastin matrix treated at 37°C for 96 h) and E96/BMP (defect filled with elastin matrix treated at 37°C for 96 h plus BMP). The animals were killed after 6 weeks. In the histological and microtomographic analysis, all groups showed bone growth from the defect margins remaining in this region without a marked inflammatory process, but in the E96/BMP group the lamellae were thicker and the collagen fibers more organized. Histometrically, the same group presented higher percentage of new formation (43.25 ± 3.72) in relation to the other groups. It was concluded that the support and delivery system formed by the elastin matrix associated with BMPs had a positive effect on the bone repair process.

Keywords: Bone regeneration, bone repair, osseointegration, elastin, morphogenetic protein

Introduction

After injury or fracture, bone tissue is able to regenerate under adequate biological and biomechanical conditions. However, this natural process might be compromised in cases of major cranial traumas or oral diseases accompanied by bone loss, which require biological and structural support for anatomical and functional recovery [1-4]. In these situations, the use of bone grafts or substitutes, which can be autologous (gold standard), homologous/allogenous or synthetic, is necessary [3, 5].

The main limitations of autologous grafts are their limited availability, need for a second procedure, and risk of complications at the donor site. Homologous and heterologous grafts are widely available but may trigger an immunogenic response and can transmit diseases such as hepatitis and human immunodeficiency virus (HIV) [6, 7]. Thus, tissue engineering has developed scaffolds for bone tissue regenerative therapies.

Currently, the use of biomaterials has become increasingly important in the medical and dental areas for the restoration of areas with bone loss or defects to prevent the consequent impairment of function and morphology and permit the repair of biological tissues [8]. Within this context, synthetic bone substitutes have

emerged as suitable alternatives because of advantages such as wide availability, absence of immunogenicity, adhesion to other substances and biodegradation, characteristics observed for polymer matrices composed of collagen and elastin [2]. In addition, the activity of these materials can be regulated by the combination with bone morphogenetic proteins (BMPs), which have osteoinductive and osteoconductive capacity [2].

Bone morphogenetic proteins are non-collagen glycoproteins found in the extracellular bone matrix, which participate with other signaling molecules (cytokines, metalloproteinases, platelet- and fibroblast-derived growth factors, insulin-like growth factor) in the process of bone healing. However, BMPs are present in limited amounts and are therefore obtained by genetic recombination [9]. Suitable recombinant BMPs are rhBMP-2 and rhBMP-7. Both proteins present osteogenic properties and are considered the most potent inducers of bone repair.

Elastin is found in the extracellular matrix and is the most abundant protein in tissues such as blood vessels, skin, lung, and elastic ligaments [10-13]. Elastin matrices are indicated for guided bone regeneration therapy because of their excellent cytocompatibility [14]. Considering these properties, polymeric biomaterials are an alternative in craniomaxillofacial reconstruction surgeries, considering the different challenges faced by specialists regarding the best treatment for severe injuries resulting from congenital and acquired anomalies, extensive bone tumor resection, sequelae of bone infections, and comminuted fractures accompanied by bone mass loss [15].

Therefore, due to the lack of biological evaluation of this new biopolymer, it was decided to carry out this study with the aim of analyzing the use of a new elastin polymer matrix combined with BMP for the repair of cranial defects in rats.

Materials and methods

Biomaterials-elastin matrix

All elastin matrix samples were obtained from São Carlos Institute of Chemistry, University of São Paulo (IQSC/USP), and were sterilized with ethylene oxide (EO) by Acecil (Sterilization Central Com. Ind. Ltda, SP, Brazil).

Biomaterials-rhBMP-2

The recombinant human Bone Morphogenetic Protein-2 (rhBMP-2, known as dibotermin alfa) was obtained commercially from R & D System, Inc. brand, (Minneapolis, MN, USA).

Preparation of the elastin matrix

Bovine auricular cartilage was washed in 0.9% saline (NaCl) and distilled water. This cartilage was treated with an alkaline solution containing salts (sulfate and chloride) and hydroxides of alkaline metals and alkaline earth metals. The treatment duration was 96 h at a temperature of 37°C and 24 h at a temperature of 50°C. In both cases, the cartilage was equilibrated after treatment in another solution containing Na^+, K^+ and Ca^{2+} sulfates and chlorides. Excess salts were removed by washes in 3% boric acid and deionized water, followed by washes in 0.3% EDTA and deionized water. The resulting material was an elastin matrix that was balanced in phosphate-buffered saline, pH 7.4, for 24 h. The matrix was then exhaustively washed with deionized water, frozen, and lyophilized. Samples measuring 5 mm in diameter were cut from the elastin matrix and some specimens were analyzed by scanning electron microscopy (SEM) to determine the pore size and elastin fiber arrangement on the matrix surface (**Figure 1C**).

Scanning electron microscopy

Photomicrographs were obtained from the matrix surface sputter-coated with gold in a Bal-Tec MED 020 Coating System (Bal-Tec, Liechtenstein). The specimens were analyzed under a Zeiss Leo 440 microscope (Cambridge, England) equipped with an Oxford detector (model 7060), operating with an electron beam of 20 kV. The pore size of the matrices was determined on the ImageJ software (50 measurements per matrix at 500× magnification) using Martin's diameter approximation [16].

Experimental design

Thirty male Wistar rats (*Rattus norvegicus*) with 12 weeks of age and mean body weight of 330 g were used (**Figure 1A**, **1B**). The animals were kept in the Animal Laboratory of the Medical College of Jundiaí at a controlled temperature (23 ± 1°C) under a 12/12-h light/dark cycle and received balanced food (Purina, Brazil) and

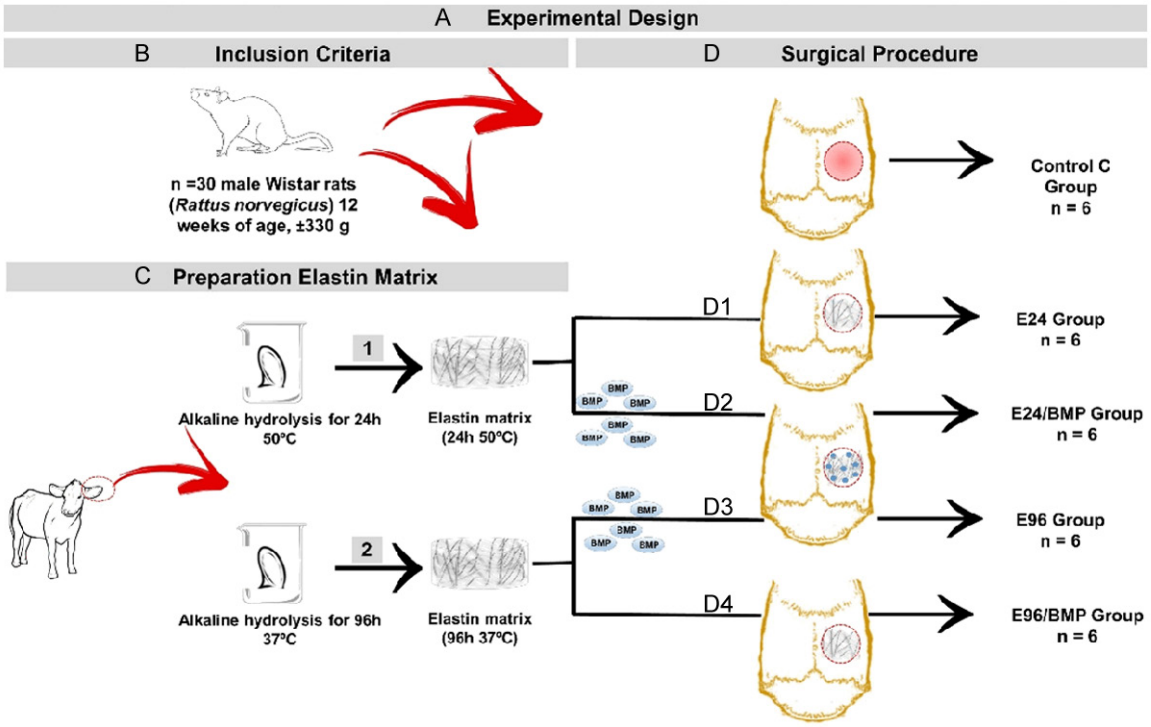

Figure 1. Schematic figures illustrating the study experimental design (A). Random allocation and inclusion criteria: Thirty male Wistar rats (*Rattus norvegicus*) with 12 weeks of age and mean body weight of 330 g were used (B). Preparation of the elastin matrix (C). The treatment duration was 96 h at a temperature of 37 °C and 24 h at a temperature of 50 °C (1 and 2 respectively). Surgical Procedure (D): The animals were submitted to an experimental surgery for creation of a cranial defect and divided into five groups of six animals each: (D) control, C-without graft; (D1) E24-graft with elastin matrix submitted to alkaline hydrolysis for 24 h at 50 °C; (D2) E24/BMP-elastin matrix treated for 24 h at 50 °C plus BMP; (D3) E96-elastin matrix submitted to alkaline hydrolysis for 96 h at 37 °C; (D4) E96/BMP-elastin matrix treated for 96 h at 37 °C plus BMP.

water *ad libitum*. The study was approved by the Institutional Review Board on Animal Use of the Medical College of Jundiai (Protocol No. 56/2015). The animals were submitted to experimental surgery for creation of a cranial defect and divided into five groups of six animals each: control, C-without graft; E24-graft with elastin matrix submitted to alkaline hydrolysis for 24 h at 50°C; E24/BMP-elastin matrix treated for 24 h at 50°C plus BMP; E96-elastin matrix submitted to alkaline hydrolysis for 96 h at 37°C; E96/BMP-elastin matrix treated for 96 h at 37°C plus BMP (**Figure 1D**).

Surgical technique for creation of cranial defect

The animals were anesthetized by gluteal intramuscular injection of a solution of ketamine 50 mg/kg i.m. (Dopalen™, Ceva, Paulínia, SP, Brazil) and Xylazine 10 mg/kg i.m. (Anasedan™, Ceva, Paulínia, SP, Brazil) in the proportion of 1:1 at a dose of 0.10 mg/100 g body weight. The animals were placed in ventral decubitus and the skullcap and surrounding areas were shaved. After confirmation of anesthesia, local antisepsis was performed with alcohol. A midline incision was made in the skull and the skin was separated for visualization of bone. The periosteum was carefully detached to expose the left parietal bone of the animal. A defect measuring 5-mm diameter was then created with a trephine bur coupled to a low-speed handpiece (ELTEC LB-100, Eltec Elektronik AG, Mainz, Germany) under abundant irrigation with saline. After local washing with saline to remove debris, the defect was filled with the biomaterials according to the respective grafted groups. The periosteum and soft tissues were repositioned and closed with 5.0 Nylon suture (Ethicon, Johnson & Johnson, Brazil) and rifamycin spray was applied as antibiotic. During the postoperative period, the animals received subcutaneous enrofloxacin and

paracetamol diluted in water. Six weeks after surgery, the animals were killed painlessly by perforation of the diaphragm for induction of pneumothorax after intraperitoneal anesthesia with 0.3 mL/100 g of a ketamine-xylazine solution.

Collection of specimens

The cranial vaults with the lining skin were collected and fixed in 10% phosphate-buffered formalin for 48 h, and later, for radiological, macroscopic and microtomographic examination.

Macroscopic and radiological analysis

After confirmation of the animal's death, the skullcap was cut with a Taimim oscillating saw (YDJZ-IID) and photographed with a Nikon digital camera to record the macroscopic clinical conditions of the bone defect, such as the presence of purulent secretion, redness, fibrotic and cystic formations or other signs that could indicate the presence of inflammation and infection. The specimens were then radiographed using an Odel 300 mA machine at a focus of 100 mA, exposure time of 0.06 s, and radiation of 40 kV. The images were digitized with the Afga system and the integrity of bone defect and adjacent areas was evaluated.

Histotechnical processing

The specimens obtained from the defect areas were immersed in buffered formalin and decalcified in hydrogen chloride (Allkimia, Campinas, Brazil) for a period of approximately 60 days. The specimens were then subjected to standard histological processing and included in Histosec™ (Merck KGaA, Darmstadt, Germany). Semi-serial coronal cuts of 5-μm thickness were performed, prioritizing the center of the circular defect and stained with hematoxylin-eosin for the identification of original bone, new bone formation, and extracellular matrix in the defect area.

Histological and histomorphometric evaluation

The histological sections were analyzed by light microscopy (Olympus model BX50) at approximate magnifications of ×10 and ×40 in the Histology Laboratory of the Medical College of Jundiai.

For histomorphometry, the bone volume was measured at three different sites of the bone defect (anterior, middle and posterior) in all groups, to quantify new bone formation across the defect area. The volume of newly formed bone was quantified in each histologic image using the Motic Images Plus 2.0 software installed in the Motic BA310 photomicroscope. The results were transformed into percentage in relation to the total bone volume of the defect.

Statistical analysis

The percentages of newly formed bone area were calculated according to the following formula: $P_{NFB} = A_{NFB} \times 100/_{TA}$ (P_{NFB}-newly formed bone percentage; A_{NFB}-newly formed bone area; TA-total area) and values were submitted to statistical analysis using analysis of variance (ANOVA) followed by post hoc Tukey's test when the ANOVA suggested a significant difference between groups ($P<0.05$).

Analysis by computed microtomography

The specimens were scanned in a SkyScan Micro-CT 1174 (SkyScan, Aartselaar, Belgium). Each specimen was scanned at a resolution of 1304×1024 pixels, rotational step of 0.5 degree, source voltage of 50 kV, source current of 800 μA, and exposure time of 5.6 s. The images were reconstructed using the NRecon software and three-dimensional images were obtained with the CT-Vox software. Morphologic parameters of trabecular bone microarchitecture were assessed using the CTAn software. A cylindrical region-of-interest (ROI) with an axis length of 3 mm (100 slices) and diameter of 1 mm was determined by segmenting the bone from the anterior to the posterior region of the rat calvaria.

Results

Characterization of materials

The rough appearance of elastin matrices was similar for the two treatments and no macroscopic differences were observed. However, the photomicrographs showed that both matrices are rough and contain pores (**Figure 2**). The pore diameter of matrices was measured using Martin's diameter approximation [16]. The pores had irregular sizes and were distributed

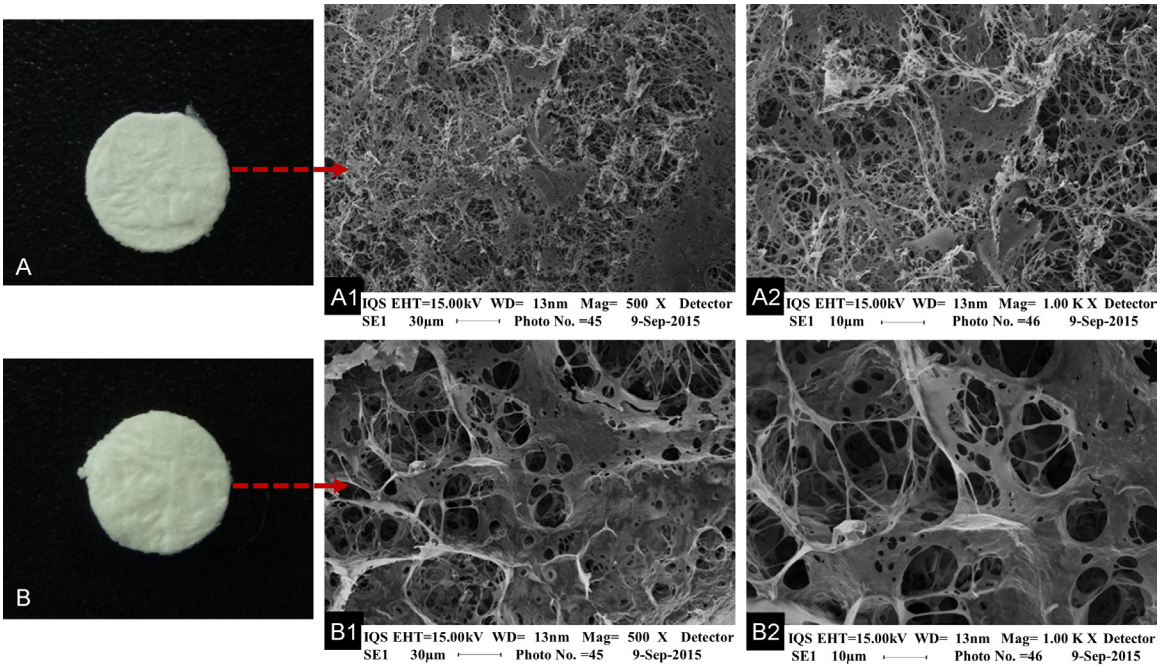

Figure 2. Macroscopic image and scanning electron microscopy of elastin matrices at different magnifications. (A) Elastin matrix treated for 24 h at 50°C; (A1) Elastin matrix treated for 24 h at 50°C (×500 magnification); (A2) Elastin matrix treated for 24 h at 50°C (×1000 magnification); (B) Elastin matrix treated for 96 h at 37°C; (B1) Elastin matrix treated for 96 h at 37°C (×500 magnification); (B2) Elastin matrix treated for 96 h at 37°C (×1000 magnification).

Table 1. Pore size of elastin matrices

MATRIX	PORE SIZE (µM)		
	Mean ± SD	Minimum	Maximum
E24	26.4 ± 9.5	12.3	68.5
E96	36.5 ± 11.2	17.3	76.0

SD: standard deviation.

in an unorganized manner. The pores of matrix E24 were smaller. This matrix was treated for a shorter period but at a higher temperature than matrix E96 (**Table 1**).

Macroscopic and radiologic analysis

Adequate skin healing was observed in all animals as demonstrated by the absence of suture dehiscence, ulcerations, and signs of wound infection. The integrity of the skullcap was maintained, with no signs of granulomas, erosions, swelling or other alterations indicating an immune reaction caused by the materials in the grafted groups (E24, E24/BMP, E96, and E96/BMP), which persisted at the graft site and were not completely resorbed. There were no radiographic signs suggesting pathologic alterations in the defect area, such as rarefaction or loss of bone integrity. The experimental bone defects showed good definition of their radiopaque margins and radiolucent center, demonstrating the sharpness of the bone defect. No immature bone formation could be identified because of its low atomic mass that does not provide sufficient radiopacity to be detected by radiographic examination (**Figure 3**).

Microtomographic analysis

The bone defect persisted in all study groups and no complete healing was observed. In the control group (C), the center of the defect exhibited no sign of bone formation with a sufficient atomic mass for visualization. In the grafted groups, images of remaining biomaterial inside the defect and formation of mineralized tissue in its center were detected, indicating osteogenesis (**Figure 4A**, **4B**).

Histological evaluation

The formation of subperiosteal bone from the original bone toward the defect center was a common finding in all groups. The newly formed bone exhibited characteristics of immature bone, including the presence of various disorganized osteocyte lacunae. However, foci of maturation of young bone showing characteris-

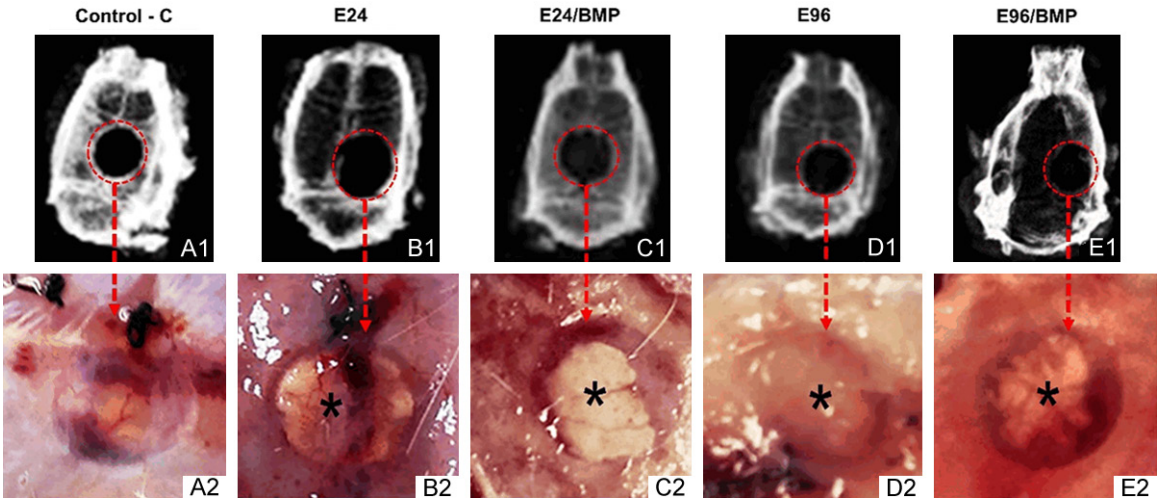

Figure 3. Radiologic and macroscopic images of the defect area in the study groups (A1-E1) and (A2-E2) respectively. (A1, A2) defect without filling, control group; (B1, B2) graft with elastin matrix submitted to alkaline hydrolysis for 24 h at 50°C (E24); (C1, C2) graft with elastin matrix treated for 24 h at 50°C plus BMP (E24/BMP); (D1, D2) graft with the elastin matrix submitted to alkaline hydrolysis for 96 h at 37°C (E96); (E1, E2) graft with elastin matrix treated for 96 h at 37°C plus BMP (E96/BMP); (A1-E1) Radiolucency at the center and radiopacity at the border of defects (low atomic mass) are observed in all experimental groups (red dashed lines); (B2-E2) Presence of the biomaterial Elastin matrix (asterisk) in the surgical bed. In all groups, there is no inflammation and infection.

tics of mature tissue were also observed. In groups E24 and E96, new bone formed in the defect center, surrounding and invaginating inside the implanted matrices. In group E96, bone formation was greater, forming a bridge and bordering the superficial and deep portions of the matrix. In group E96/BMP, the volume of young bone was more marked. This young bone occupied almost the entire defect area and connected the ends of the original bone to the defect margins, providing osseointegration. In addition, little connective tissue remained in the defect area in group E96/BMP. There were no signs of rejection in the grafted groups since no cells characteristic of an inflammatory process such as multinucleated giant cells, neutrophils or lymphocytes were observed (**Figure 5A**).

Histomorphometric evaluation

The percent volume of newly formed bone in the defect area was 7.87 ± 2.53, 24.01 ± 0.55, 31.31 ± 6.37, 19.77 ± 2.62 and 43.25 ± 3.72 in the control, E24, E24/BMP, E96 and E96/BMP groups, respectively (**Figure 5B**). Statistical analysis revealed a higher amount of newly formed bone in the grafted groups compared to control. Comparison of the grafted groups showed superior osteogenesis in the E96/BMP group, demonstrating the efficacy of BMP and alkaline treatment of the elastin matrices for 96 h.

Discussion

Advances in studies with bone substitutes have made tissue regenerative therapy a promising tool in several areas of medicine and dentistry, due to the high prevalence of craniomaxillofacial defects associated with bone loss as well as the limitations of autologous grafts [1, 2, 4, 17]. However, there is still no ideal bone substitute considering the limitations and disadvantages related to the mechanical resistance, high production cost and difficulty in maintaining the surgical area without invasion of fibroblasts coming from surrounding connective tissue [18-20].

In this context, the use of materials derived from elastin as a bone substitute has aroused interest in tissue engineering due to the remarkable characteristics of this structural protein such as tropoelastin coacervation ability, high elasticity, mechanical stability in the surgical bed and biological activity of signaling and molecular induction of peptides derived from elastin degradation [21].

The process of obtaining these biopolymers directly affects the three-dimensional arrange-

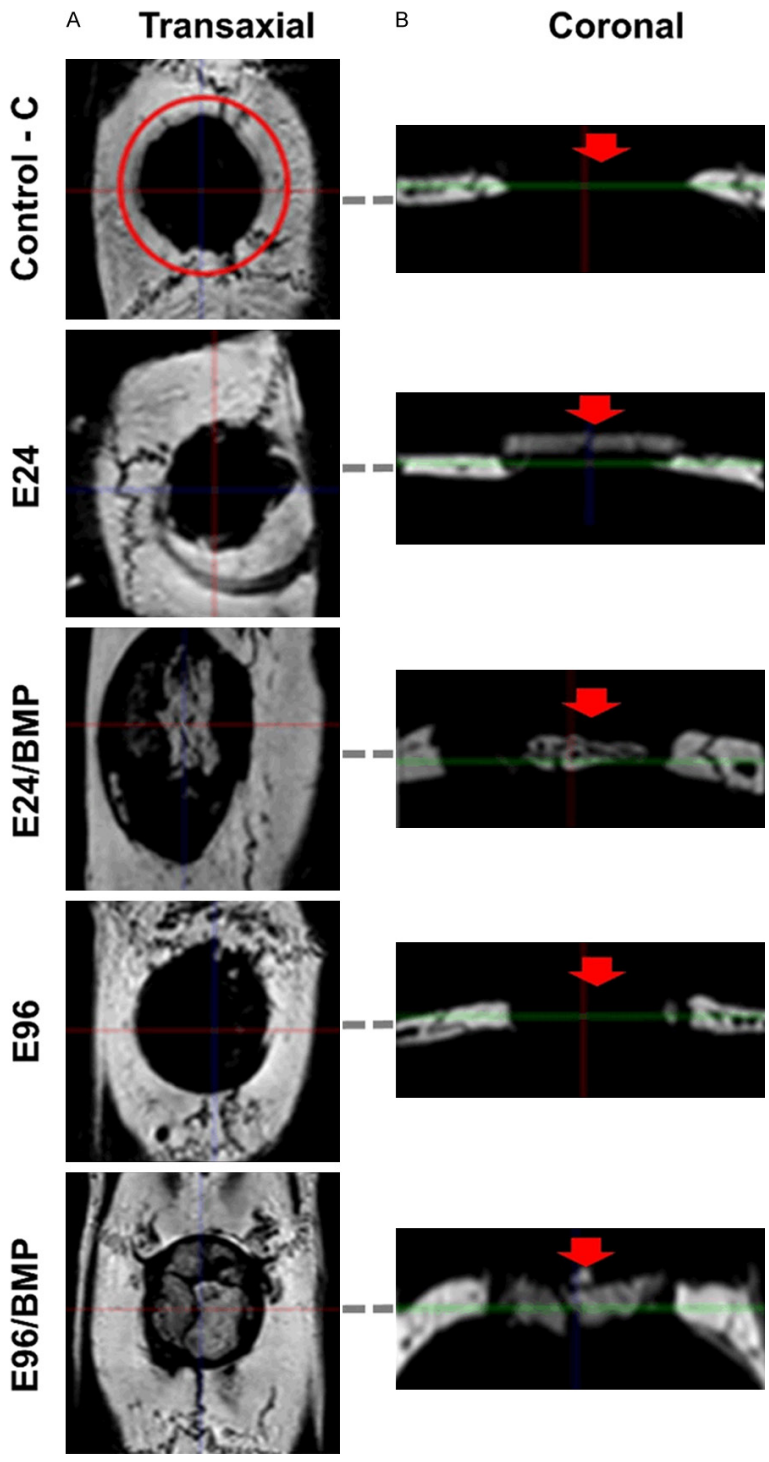

Figure 4. Micro-computed tomography (micro-CT) images of the calvaria after 6 weeks of implantation of indicated materials. 2D views of transaxial (A), coronal (B) sections. Newly regenerated bone in the C group (defect without filling), E24 group (graft with the elastin matrix submitted to alkaline hydrolysis for 24 h at 50°C), E24/BMP group (graft with the elastin matrix treated for 24 h at 50°C plus BMP), E96 group (graft with elastin matrix submitted to alkaline hydrolysis for 96 h at 37°C) and E96/BMP (graft with elastin matrix treated for 96 h at 37°C plus BMP). Bone growth is observed from the defect margins, with bone islets in groups E24, E24/BMP and E96/BMP.

ment of elastin fibers and thus the cellular support function in the medium where it is inserted. Thus, two types of collagen enzymatic thermal hydrolysis methods were proposed for the production of elastin matrices with hydrophilic and hydrophobic sites responsible for crosslinking, elasticity and cell signaling.

Therefore, the objective of this study was to analyze the use of elastin-based biomaterial derived from bovine auricular cartilage associated with bone morphogenetic protein in the repair of bone defects in calvaria of rats.

To investigate the effect of elastin matrix associated with BMP on the bone repair process, we used macroscopic, radiological, microtomography, histology and histomorphometry analyses.

In the macroscopic analysis of specimens, no inflammatory or infectious signs such as purulent secretion, abscesses, swelling and local redness were observed in any experimental group (E24, E24/BMP, E96 and E96/BMP). These results are in agreement with preliminary studies that affirm that the heterologous elastin matrix presents satisfactory biocompatibility, being a protein present in the extracellular organic matrix with the same sequence of tropoelastin genes between species [22, 23].

The results observed in histological analysis corroborate these findings, since all defects filled with the biopolymer did not present polymorphonuclear cells participating

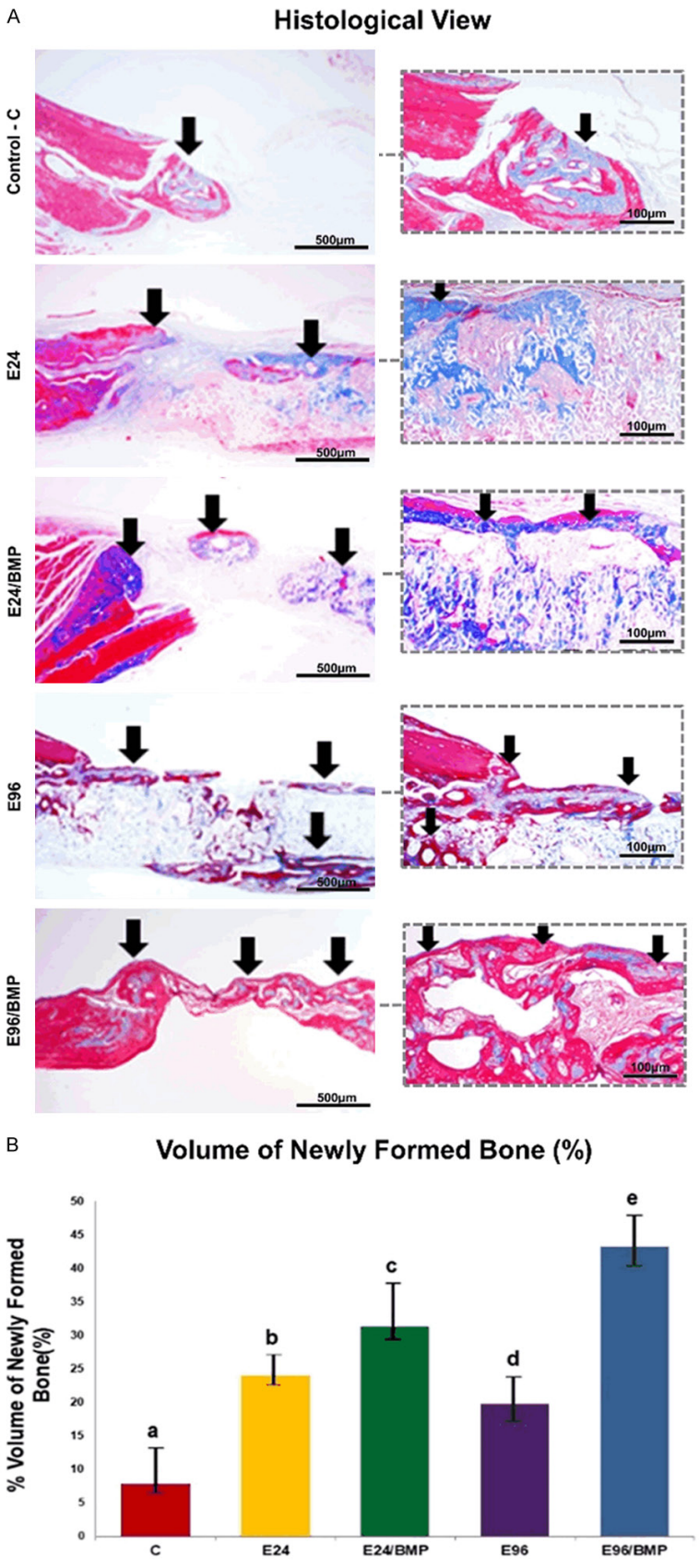

Figure 5. Histological views (A) and graphs of volume of newly formed bone (%) (B) in calvaria defects created in the animals. Note the subperiosteal new bone formation (black arrows) from the border and center of the bone defect (A). Graph of volume of newly formed bone showed higher percentage in the group filled with elastin matrix treated for 96 h at 37°C plus BMP (E96/BMP) in relation to the other experimental groups (B). N = 6/group different letters indicate statistically significant difference between groups ($a \neq b \neq c \neq d \neq$, $P<0.05$). (HE; original magnification ×10; bar = 500 µm and Insets, magnified images ×40; bar = 100 µm).

in the immune system. Thus, it is suggested that the two processes of extraction by thermal hydrolysis of elastin, alkaline hydrolysis at 50°C for 24 h and 37°C for 96 h, did not present residual products, due to its degradation, which causes pH alteration of the surrounding environment, thus inducing exaggerated inflammatory responses [19, 24-28].

Another relevant point that contributed to these results was the choice of elastin eliciting method. Alkaline treatment and sterilization by ethylene oxide promoted acellularization of the bovine material and removal of its impurities, which makes this biopolymer non-toxic and a promising alternative in therapies for bone reconstruction [19, 29].

In the histological, radiological and microtomographic images, it is possible to observe that no specimen presented complete closure of the defect by mature bone tissue. Bone growth occurred centripetally, from the edges of the surgical

wound remaining in this region, and in defects filled with biopolymer there was still presence of elastin at experiment completion. These characteristics are in agreement with studies dealing with critical-size defects that do not spontaneously regenerate [30, 31]. However, the E96/BMP group presented trabecular conformation in some central regions, thick lamellae adjacent to the defect margin and predominance of more organized collagen fibers.

Histomorphometrically, the E96/BMP group had higher percentage of new bone formation (43.25 ± 3.72) in relation to the other experimental groups, C, E24, E24/BMP, E96 and E96/BMP (7.87 ± 2.53, 24.01 ± 0.55, 31.3 ± 6.37, 19.77 ± 2.62) respectively. This finding can be attributed to the alkaline treatment time of the biopolymer, 96 h, thus increasing the porosity, three-dimensional arrangement of the elastin fiber and hydrophobic and hydrophilic capacity. Thus, it facilitated cell proliferation and differentiation, and angiogenesis as suggested by the studies of Billstrõm [32] and Yeo [33]. In addition, the association with Bone Morphogenetic Proteins (BMPs) potentiated the osteogenic effect of the three-dimensional structure [18, 34].

Concomitantly to the higher percentage of new bone formation observed in the E96/BMP group, the resorption rate was also higher in relation to the other groups at experiment completion. The studies of Cunha [2] had the same results in osteotomies of femurs of rats with 60 days of treatment with polyanionic acellular matrices of collagen, showing that the biomaterial resorption occurred properly, exerting its support function during the regeneration process [35].

However, there is still controversy in the scientific literature regarding the optimal time for alkaline treatment of these biomaterials. Thus, other studies on the three-dimensional structure of elastin polymer matrices are necessary, as well as investigation of pore interconnectivity and characterization of surface hydrophilicity/hydrophobicity. As a perspective for future studies, the use of complementary therapies can be analyzed to accelerate and increase the process of new bone formation, such as the use of low-intensity ultrasound [36] and photobiomodulation therapy with the use of low-level laser [5, 37].

Conclusion

Elastin polymer matrices derived from bovine auricular cartilage exhibit bone regenerative capacity and can accelerate local osteogenesis when combined with BMP, suggesting their possible use in craniomaxillofacial regenerative therapies.

Acknowledgements

The authors are grateful to the Institute of Chemistry of São Carlos (IQSC/USP), Department of Biological Sciences (Anatomy) and Department of Dentistry, Endodontics and Dental Materials, Bauru School of Dentistry, University of São Paulo (USP), NAPED (Research and Teaching Support Center, Medical School of Jundiai, FMJ), and Cruzeiro do Sul University-CEUNSP.

Disclosure of conflict of interest

None.

Address correspondence to: Marcelo Rodrigues da Cunha, Department of Morphology and Pathology, Medical College of Jundiai, São Paulo, Rua Francisco Telles, 250 Vila Arens, CEP, 13202-550, Cx. Postal 1295, Jundiaí-SP, Brazil. Tel: (55 11 33952100); Fax (55 11 33952100); E-mail: cunhamr@hotmail.com

References

[1] Sen MK, Miclau T. Autologous iliac crest bone graft: should it still be the gold standard for treating nonunions? Injury 2007; 38: 2-7.

[2] Cunha MR, Santos AR, Goissis G, Genari SC. Implants of polyanionic collagen matrix in bone defects of ovariectomized rats. J Mater Sci Mater Med 2008; 19: 1341-1348.

[3] Mauffrey C, Seligson D, Lichte P, Pape HC, Al-Rayyan M. Bone graft substitutes for articular support and metaphyseal comminution: what are the options? Injury 2011; 42: S35-S39.

[4] Egol K, Nauth A, Lee M, Pape H, Watson J, Borrelli JJ. Bone grafting: sourcing, timing, strategies, and alternatives. J Orthop Trauma 2015; 29: S10-S14.

[5] de Oliveira Gonçalves JB, Buchaim DV, de Souza Bueno CR, Pomini KT, Barraviera B, Júnior RSF, Andreo JC, de Castro Rodrigues A, Cestari TM, Buchaim RL. Effects of low-level laser therapy on autogenous bone graft stabilized with a new heterologous fibrin sealant. J Photochem Photobiol B 2016; 162: 663-668.

[6] Kretlow J, Mikos A. 2007 AIChE alpha chi sigma award: from material to tissue: biomaterial

development, scaffold fabrication, and tissue engineering. AIChE J 2008; 54: 3048-3067.
[7] Vagaská B, Bačáková L, Filová E, Balík K. Osteogenic cells on bio-inspired materials for bone tissue engineering. Physiol Res 2010; 59: 309-322.
[8] Buchaim RL, Andreo JC, Rodrigues AC, Buchaim DV, Dias DV, Daré LR, Roque DD, Roque JS. The action of demineralized bovine bone matrix on bone neoformation in rats submitted to experimental alcoholism. Arq Bras Med Vet Zootec 2013; 65: 715-721.
[9] Wozney JM, Rosen V, Celeste AJ, Mitsock LM, Whitters MJ, Kriz RW, Hewick RM, Wang EA. Novel regulators of bone formation. Science 1988; 44: 387.
[10] Pasquali-Ronchetti I, Baccaeani-Contri M. Elastic fiber during development and aging. Microsc Res Tech 1997; 38: 428-435.
[11] Faury G. Function-structure relationship of elastic arteries in evolution: from microfibrils to elastin and elastic fibres. Pathol Biol 2001; 49: 310-325.
[12] Martyn CN, Greenwald S. A hypothesis about a mechanism for the programming of blood pressure and vascular disease in early life. Clin Exp Pharmacol Physiol 2001; 28: 948-951.
[13] Lane JM. Bone morphogenic protein science and studies. J Orthop Trauma 2005; 19: 17-22.
[14] Bozkurt A, Apel C, Sellhaus B, van Neerven S, Wessing B, Hilgers RD, Pallua N. Differences in degradation behavior of two non-cross-linked collagen barrier membranes: an in vitro and in vivo study. Clin Oral Implants Res 2014; 25: 1403-1411.
[15] Dimitriou R, Mataliotakis GI, Calori GM, Giannoudis PV. The role of barrier membranes for guided bone regeneration and restoration of large bone defects: current experimental and clinical evidence. BMC Med 2012; 10: 81.
[16] Allen T. Powder sampling and particle size determination. 2003.
[17] Oryan A, Alidadi S, Moshiri A, Maffulli N. Bone regenerative medicine: classic options, novel strategies, and future directions. J Orthop Surg Res 2014; 9: 1-27.
[18] Liu F, Porter RM, Wells J, Glatt V, Pilapil C, Evans CH. Evaluation of BMP-2 gene-activated muscle grafts for cranial defect repair. J Orthop Res 2012; 30: 1095-1102.
[19] Hirata HH, Munhoz MA, Plepis AM, Martins VC, Santos GR, Galdeano EA, Cunha MR. Feasibility study of collagen membranes derived from bovine pericardium and intestinal serosa for the repair of cranial defects in ovariectomised rats. Injury 2015; 46: 1215-1222.
[20] Gurumurthy B, Bierdeman P, Janorkar A. Composition of elastin like polypeptide-collagen composite scaffold influences in vitro osteogenic activity of human adipose derived stem cells. Dent Mater 2016; 5: 1-8.
[21] Ragnoni E, Palombo F, Green E, Winlove C, Di Donato M, Lapini A. Coacervation of α-elastin studied by ultrafast nonlinear infrared spectroscopy. Phys Chem Chem Phys 2016; 18: 27981-27990.
[22] Chung M, Miao M, Stahl R, Chan E, Parkinson J, Keeley F. Sequences and domain structures of mammalian, avian, amphibian and teleost tropoelastins: clues to the evolutionary history of elastins. Matrix Biol 2006; 25: 492-504.
[23] Ratner BD, Hoffman AS, Schoen FJ, Lemons JE. Biomaterials Science: an introduction to materials in medicine. Elsevier Academic Press 2003.
[24] Henkel J, Woodruff M, Epari D, Steck R, Glatt V, Dickinson I, Choong P, Schuetz M, Hutmacher DW. Bone regeneration based on tissue engineering conceptions-A 21st century perspective. Bone Res 2013; 1: 216-248.
[25] Rnjak-Kovacina J, Wise SG, Li Z, Maitz PK, Young CJ, Wang Y, Weiss AS. Tailoring the porosity and pore size of electrospun synthetic human elastin scaffolds for dermal tissue engineering. Biomaterials 2011; 32: 6729-6736.
[26] Rosa F, Lia R, de Souza K, Goissis G, Marcantonio EJ. Tissue response to polyanionic collagen: elastin matrices implanted in rat calvaria. Biomaterials 2003; 24: 207-212.
[27] Miguel FB, Barbosa Júnior Ade A, de Paula FL, Barreto IC, Goissis G, Rosa FP. Regeneration of critical bone defects with anionic collagen matrix as scaffolds. J Mater Sci Mater Med 2013; 24: 2567-2575.
[28] Da Luz Moreira P, Genari SC, Goissis G, Galembeck F, An YH, Santos AR. Bovine osteoblasts cultured on polyanionic collagen scaffolds: an ultrastructural and immunocytochemical study. J Biomed Mater Res B Appl Biomater 2013; 101: 18-27.
[29] Machado EG, Issa JP, Figueiredo FA, Santos GR, Galdeano EA, Alves MC, Chacon EL, Ferreira Junior RS, Barraviera B, Cunha MR. A new heterologous fibrin sealant as scaffold to recombinant human bone morphogenetic protein-2 (rhBMP-2) and natural latex proteins for the repair of tibial bone defects. Acta Histochem 2015; 117: 288-296.
[30] Gosain A, Song L, Yu P, Mehrara B, Maeda C, Gold L, Longaker M. Osteogenesis in cranial defects: reassessment of the concept of critical size and the expression of TGF-beta isoforms. Plast Reconstr Surg 2000; 106: 360-371.
[31] Pomini KT, Cestari TM, Santos German ÍJ, de Oliveira Rosso MP, de Oliveira Gonçalves JB, Buchaim DV, Pereira M, Andreo JC, Rosa GM

Júnior, Della Coletta BB, Cosin Shindo JVT, Buchaim RL. Influence of experimental alcoholism on the repair process of bone defects filled with beta-tricalcium phosphate. Drug Alcohol Depend 2019; 197: 315-325.

[32] Billström GH, Blom AW, Larsson S, Beswick AD. Application of scaffolds for bone regeneration strategies: current trends and future directions. Injury 2013; 44: S28-S33.

[33] Yeo GC, Aghaei-Ghareh-Bolagh B, Brackenreg EP, Hiob MA, Lee P, Weiss AS. Fabricated elastin. Adv Healthc Mater 2016; 4: 2530-2556.

[34] Venkatesan J, Kim SK. Chitosan composites for bone tissue engineering-an overview. Mar Drugs 2010; 8: 2252-2266.

[35] Yu X, Tang X, Gohil S, Laurencin C. Biomaterials for bone regenerative engineering. Adv Heal Mater 2015; 118: 6072-6078.

[36] Pomini KT, Andreo JC, Rodrigues Ade C, de O Gonçalves JB, Daré LR, German IJ, Rosa GM Jr, Buchaim RL. Effect of low-intensity pulsed ultrasound on bone regeneration biochemical and radiologic analyses. J Ultrasound Med 2014; 33: 713-717.

[37] Pomini KT, Buchaim DV, Andreo JC, Rosso MPO, Della Coletta BB, German ÍJS, Biguetti ACC, Shinohara AL, Rosa Júnior GM, Cosin Shindo JVT, Alcalde MP, Duarte MAH, de Bortoli Teixeira D, Buchaim RL. Fibrin sealant derived from human plasma as a scaffold for bone grafts associated with photobiomodulation therapy. Int J Mol Sci 2019; 20.